SSRG International Journal of Material Science and Engineering
ISSN: 2394 – 8884 / https://doi.org/10.14445/23948884/IJMSE-V8I3P102

Volume 8 Issue 3, 6-13, Sep-Dec 2022

Original Article

Synthesis and Characterization of ZnS Nanoparticles by Ball Milling Technique

Simon K. Ologundudu[1], Azubuike J. Ekpunobi[2], Imosobomeh L. Ikhioya[3]

[1,2]*Department of Physics and Industrial Physics, Nnamdi Azikiwe University, Awka, Anambra State, Nigeria.*
3Department of Physics and Astronomy, University of Nigeria, Nsukka, Enugu State, Nigeria

Received: 01 November 2022 Revised: 02 December 2022 Accepted: 16 December 2022 Published: 31 December 2022

Abstract *- Zinc sulphide (ZnS) nanoparticles were produced utilizing a mechanical milling technique. The mechanical approach was chosen for synthesising ZnS nanoparticles due to its simplicity, ability to produce material at ambient temperature, lack of need for expensive apparatus, and inexpensive cost. X-ray diffraction (XRD), atomic absorption spectroscopy (AAS), scanning electron microscopy (SEM), UV-visible spectroscopy, energy dispersive analysis (EDAX), and four-point probe were used to evaluate the produced ZnS nanoparticles. The ZnS nanoparticles' XRD measurements reveal peaks at the crystal plane (111), (220), (320), and (321). It was found that ZnS's optical energy band gap increased from 3.72 eV to 4.02 eV. The absorbance of ZnS nanoparticles shows moderate absorbance values in the UV region but dramatically decreases as they move towards the visible and near-infrared regions. ZnS nanoparticles include 41.46 percent Zn, 36.79 percent C, 18.81 percent S, and 2.94 percent Fe, according to chemical analysis of their composition. The sheet resistance, resistivity, and conductivity were measured and found to be 4.83 × 107 Ω/Sq., 10.85 Ω.cm and 9.2 × 10-2 (Ω.cm)-1, respectively. ZnS nanoparticles are classified as promising materials for various optoelectronic devices based on their determined properties.*

Keywords *- Zinc, Ball milling technique, X-ray diffraction, Surface morphology, Optical.*

1. Introduction

Zinc sulphide nanoparticles represent an extremely significant material that has been thoroughly researched; infrared windows, Photonics, light-emitting diodes sensors, nonlinear optical devices, Catalysis, flat panel displays field emitters, and lasers are just a few of the numerous applications it is appropriate for Cubic sphalerite is the most prevalent and stable Zinc sulphide polymorph. Still, hexagonal wurtzite becomes more stable beyond 1023°C [1]. A coprecipitation technique can also be used to create a body-centered tetragonal phase that theoretical models have previously anticipated. According to an exhaustive review by Fang et al. [2-4]. Nanomaterials are able to improve Due to their size-dependent characteristics at this scale, a variety of industrial items' performance and shelf life. The most fundamental element in the creation of a nanostructure is a nanoparticle. Nanotechnology is the study of altering matter at atomic and molecular size. A nanoparticle can be any size between 1 and 100 nm. The creation of a theory to explain various physical phenomena that came later, following the development of analytical tools, led to the current technology that works with nanoparticles or simply nanotechnology [5]. Other than a nanoparticle's optical quality, certain phenomena (chemical and physical characteristics) have opened up new opportunities in a variety of industries, such as semiconductors. Several categories are used to categorize semiconductors. Ionic semiconductors, compound semiconductors based on the atoms that make them up, elemental Semiconductors are based on their nature, and finally, amorphous, polycrystalline, or single-crystal semiconductors depending on their structure [16]. They have an electrical resistance that falls off typically exponentially with temperature and is halfway between that of metals and insulators. Materials from group IV of the periodic table, a combination of group III and group V (referred to as III-V semiconductors), or combinations of group II and group VI make up the semiconductors' atoms. Because semiconductors are made up of elements from different periodic table groups, their characteristics vary [7].

One of the earliest semiconductors to be found, ZnS, has exceptional features that can be used for a variety of purposes, such as field emitters, electroluminescence, electrocatalysts, and biosensors. The anomalous physical and chemical properties of nano ZnS in comparison to bulk ZnS include enhanced surface-to-volume ratio, quantum size effect, surface and volume effect, macroscopic quantum tunneling effect, more optical absorption, chemical activity, thermal resistance, catalysis, and low melting point [25]. ZnS has received much attention for this application because of its great chemical stability, non-toxicity, and eco-friendliness. It has two crystalline forms at room temperature: sphalerite, which has a bandgap of 3.6 eV, and wurtzite (hexagonal phase), which has a band gap of 3.77 eV [9]. Natural ZnS material typically contains a sizeable quantity of impurity, which influences the physical and optical properties and prevents reproducible characterization. Due to impurities and flaws in the crystal formations, there is some variance in the lattice constants of both cubic and hexagonal structures [10].

Photoconductors, solar panels, modulators, sensors, photocatalytic, optical coatings, transducers, and optoelectronic applications are a few examples of the many potential uses for ZnS [11-24].

In this investigation, ball milling methods were used to produce ZnS. The concentration of elements in a given sample of ZnS nanoparticles was evaluated using atomic absorption spectroscopy. Using SEM, the material's morphology was examined. The materials' structural investigation and elemental composition were done using the XRD findings and EDX, respectively. The four-point probe was used to examine the electrical characteristics of ZnS. Using UV-Vis spectroscopy, the optical characteristics and bandgap energy were investigated.

2. Materials and Method

2.1. Synthesis of ZnS Nanoparticles

ZnS nanoparticles were produced using the mechanical milling process. The sample of ZnS ore was ground to nano sizes ranging from 0-100 nanometers in a 5-kilogram laboratory ball mill. Reagents Employed to prepare the aqua ragia for the samples' acid digestion, the following chemicals were used: deionized water, hydrochloric and nitric acids, and hydrochloric acid. Sample Gathering Sphalerite (ZnS) ore from the Abakaliki, Enyigba mining location in Nigeria Ebonyi State was used in this investigation.

2.2. Sample Preparation for AAS Analysis Procedures

This digesting technique, which does not aim to decompose the sample completely, is based on EPA method 3052 and the China National Standard to extract the elements from soil samples. Soil samples weighing around 2g were placed directly into 100 mL polypropylene (PP) reaction containers. Each sample was supplemented with 70 percent HCl and 30 percent HNO_3 (both concentrated), the same acid mixture used as the benchmark for soil sample digestion. Also created were analytical reagent blanks that just contained the acids. The lids were lightly placed over the jars before they were set into the block. The materials were digested for one hour at 120^{o}C. Following digestion, the digested sample solutions were chilled and diluted with deionized water to a final volume of 100.0 mL before being filtered. Analysis of the filtrate solution was now possible. Using a Buck Scientific AAS 211, the Atomic Absorption Spectroscopy study was carried out.

2.3 Characterization of ZnS nanoparticles

The morphology of the materials was examined using a scanning electron microscope (SEM). The lattice crystal and peak intensities were investigated using Bruker D8 Advance XRD with Cu K line = 1.54056 in the 2theta range from 15^{o} to 80^{o}. The elemental analysis of a sample performs using EDX and a Buck 210/211ATS Compact Spectrometer to determine the concentration of metallic elements in the given sample. The optical characteristics of the nanoparticles were investigated using a Schimadzu UV-1800 visible spectrophotometer in the UV-visible range. The electrical characteristics of nanoparticles were examined using the outdated Jandel four-point probes (model TY242MP) approach.

3. Results and Discussion

3.1. Atomic Absorption Spectroscopy Analysis

Using Atomic Absorption Spectroscopy, Table 1 displays the concentration of metallic atoms found in ZnS nanoparticles. According to the AAS analysis, the sample of ZnS nanoparticles contains 415g/kg of Zn while also including trace amounts of other metals, such as minor elements like Iron and Copper.

Table 1. AAS Analysis of ZnS nanoparticles

	ZnS Nanoparticles
Zinc (Zn) g/kg	415g/kg
Iron (Fe) g/kg	1.09g/kg
Copper (Cu) g/kg	0.13g/kg

3.2. Surface morphological investigation of ZnS nanoparticles

SEM is mostly used to research surface features or sample topography; hence it is used to analyze the surface morphology of ZnS nanoparticles. The University of Cape Town used Scanning. Electron Microscope Carl Zeiss EVO 18 instrument to characterize ZnS nanoparticles.

According to the SEM microstructural investigation, the produced ZnS comprises crystallites shaped like regular grains of ZnS nanoparticles [2]. The surface micrograph of the ZnS nanoparticle characterized with 500 nm shows a large nanoparticle compared to the one done with 1 µm and 2 µm as shown in figure 1

3.3 Structural Analysis of ZnS nanoparticles

The X-ray diffraction analysis provides fundamental information about crystallographic planes' crystal structure, flaws, and miller indices. A characteristic of the substance that aids in identifying its structure is the diffraction pattern, which consists of the positions and intensities of the diffraction peaks. We can determine the unit cell's structure, size, shape, and orientation by analyzing the diffraction peaks. Structural investigation of ZnS nanoparticles was accomplished by employing an X-ray powder diffractometer (XRD) with a Cu-Kα radiation source (λ = 1.5406 Å). Figure 2 displays the ZnS nanoparticles' XRD diffraction pattern. The preferred orientations of the nanoparticles were (111), (112), 220), (320), and (321), and distinct peaks of the nanoparticles were seen at 20.46^{o}, 21.86^{o}, 31.33^{o}, 44.09^{o}, and 52.98^{o}. Because contaminants might have created them in the sample, some XRD peaks are left out without indexing.

Fig. 1 SEM micrographs of ZnS nanoparticles

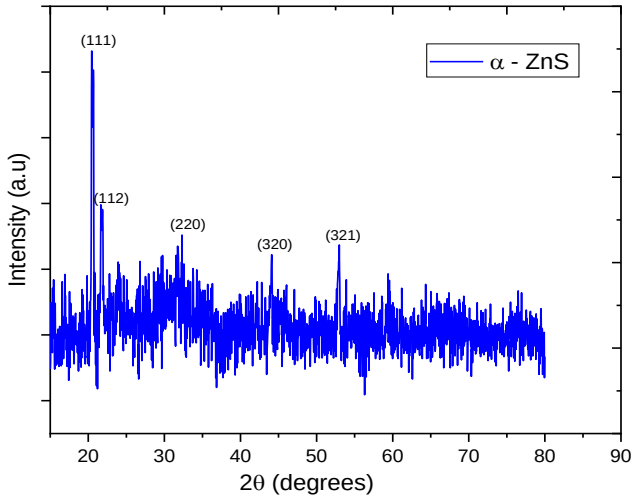

Fig. 2 X-Ray Diffraction pattern for ZnS nanoparticles.

Table 2. Structural parameters

2θ (degree)	Spacing d(Å)	Lattice constant (Å)	FWH, β	Hkl	Crystallite Size, D (nm)	Dislocation density, δ m^2
20.46	4.336	7.511	0.342	111	0.411	1.753
21.86	4.062	8.124	0.206	112	0.685	6.151
31.33	2.852	5.704	0.248	220	0.580	8.708
44.09	2.052	4.588	0.259	320	0.577	8.590
52.92	1.728	4.234	0.262	321	0.591	8.576

Table 3. Atomic weight

Element Number	Element Symbol	Element Name	Wt%
30	Zn	Zinc	41.46
16	S	Sulfur	18.81
6	C	Carbon	36.79
26	Fe	Iron	2.94

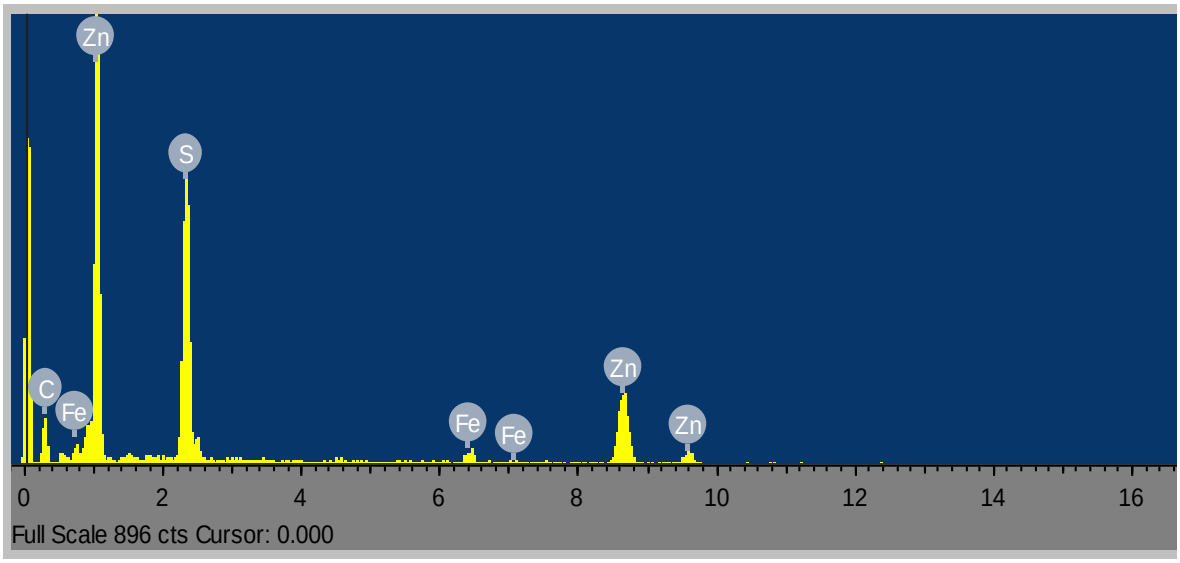

Fig. 3 EDX spectrum of ZnS nanoparticles.

Given that the peaks are relatively broad, the nanoparticles must be quite small [1-2,7]. The indexed peaks corroborate that the ZnS nanoparticles have a spherically cubic (blend) shape. Based on the diffraction peaks' full width at half maximums (FWHM), the average crystallite sizes were calculated using the Debye-Scherrer equation [7, 17]. The XRD spectrum demonstrated the nanoparticle's polycrystalline composition. Planes (111), (112), (220), (320), and (321), which correspond to angles of 20.46°, 21.86°, 31.33°, 44.09°, and 52.98°, respectively, show diffraction peaks in the pattern. The material's computed structural characteristics are shown in Table 1. It was found that as the 2-theta angle material rises, the crystallite size and the lattice parameters grow.

$$D = \frac{K\lambda}{\beta Cos\theta} \quad (1)$$

3.4. Elemental Composition of ZnS Nanoparticle

Figure 3 displays the results of an energy-dispersive X-ray investigation of ZnS nanoparticles. According to the EDX study, the ZnS nanoparticles are mostly made of zinc, sulfur, carbon, and a minimal amount of iron. The compound makeup of all the constituent elements was disclosed by the EDX [1-2,7]. The chemical composition of ZnS was determined by energy dispersive X-ray (EDX) analysis to be primarily 41.46% Zn, followed by 36.79%C, 18.81% S, and 2.94% Fe (Table 3).

3.5 Optical analysis of ZnS Nanoparticles

The absorbance result of ZnS nanoparticles dispersed in distilled water and ethanol is shown in Figure 4a. When ZnS was dissolved in distilled water or ethanol, the absorbance in the UV part of the spectrum was moderate (40%) at wavelengths of 322 nm and 349 nm, respectively, before dropping sharply to 1%. In the visible portion of the spectrum, the ZnS nanoparticles in distilled water showed a slight increase of 5%, which decreased as they proceeded into the NIR region of the spectrum. The ethanol-dissolved ZnS showed a shallow pattern in the visible spectrum that diminished as it proceeded into the NIR range. ZnS nanoparticles' spectra exhibit a strong absorbance in the ultraviolet, but a low absorbance in the visible area [2]

The transmittance of distilled and ethanol-dissolved ZnS nanoparticles increases from 40 to 98 percent in the UV-visible region of the spectrum, followed by a shallow fall in the visible area, as can also be seen in Figure 4b. The enhanced scattering of photons by crystal defects caused by impurities could cause a decrease in transmittance in the visible region between the wavelengths of 392-750 nm. As seen in Figure 4c, the ZnS nanoparticle likewise displayed poor reflectivity within the visible spectrum. It makes them a better material to utilize as a window layer during the construction of solar cells [7]

According to Jothibas et al. [9], the following relation can be used to compute the optical band gap with direct transition: $A(h\text{-}Eg)^n = \alpha h\nu$ Where n is a number that describes the transition process, and hv is the photon energy, A is a constant that depends on the transition probability, is the absorption coefficient, Eg is the optical band gap, and n =1/2 and 3/2 for direct allowed and forbidden transitions, respectively, and n =2 and 3 for indirect allowed and forbidden transitions, respectively. We take n = 1/2 in our case to get the optical bandgap using the following relationship for the direct permitted transition: $\alpha h\nu = A(h\nu\text{-}Eg)^{1/2}$

By plotting $(\alpha h\nu)^2$ versus hv and then extrapolating the straight line of the Tauc plots, as seen in Figure 4d, the direct band gap of the samples was determined. The curve in Figure 4d was used to calculate the ZnS nanoparticle sample's optical band gap value. It was discovered that the optical band gap increased from 3.72 eV to 4.02 eV. This band gap value is a good indicator of how much blue-shifted ZnS nanoparticles are compared to bulk (340 nm, Eg = 3.7 eV). ZnS nanoparticles' rising bandgap energies may be proof of the quantum confinement effect brought on by structures getting smaller [9]

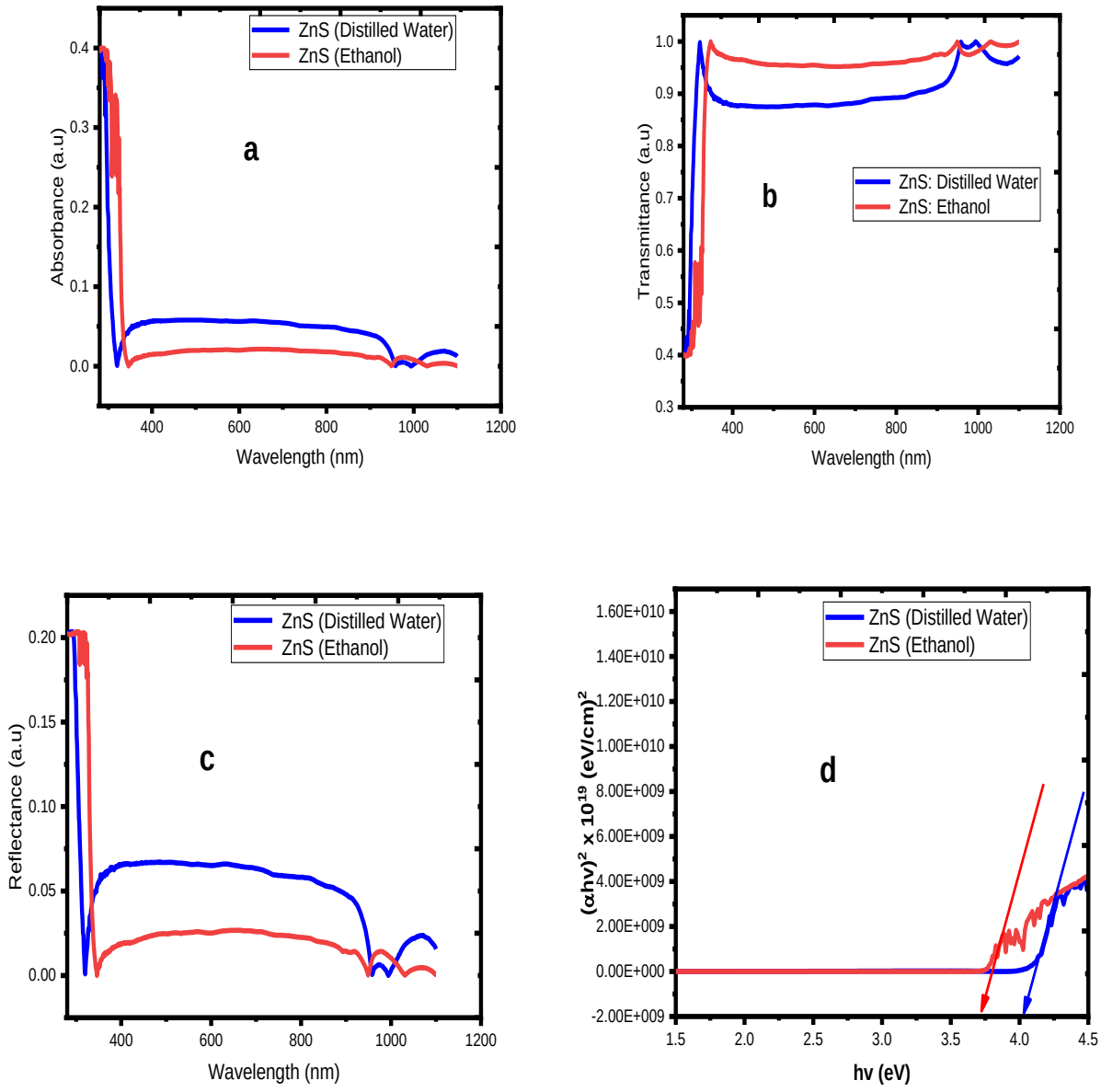

Fig. 4 Absorbance spectra of ZnS nanoparticles (a), Transmittance spectra of ZnS nanoparticles (b), Reflectance spectra of ZnS nanoparticles (c), and Optical energy bandgap plots of ZnS nanoparticles (d)

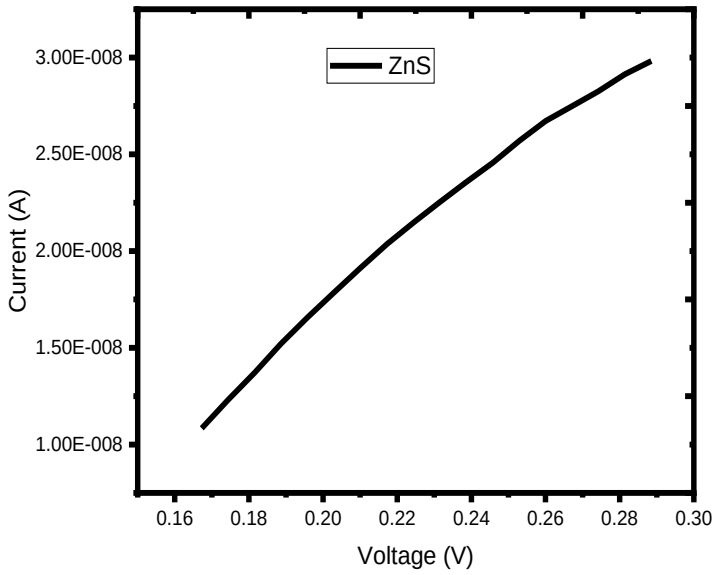

Fig. 5 I-V characteristic of ZnS nanoparticles

3.6. Electrical Properties

The electrical (I-V) measurement of ZnS nanoparticles was detected using the four-point probe technique. The nanoparticles were applied to a glass substrate before the electrical investigation was performed. Figure 5 shows the average current and the related voltage. We noticed that the current passing through the film rises linearly as the electrode's voltage increases. This suggests that the film has a higher conductivity, which could assist in producing solar cells with a higher frequency [13-14]. ZnS thin film was found to have an average current and voltage of 2.14×10^{-8} A and 2.28×10^{-2} V, respectively. The resistivity (ρ) was estimated using the relation [10];

$$\rho = \frac{\pi}{In2}\left(\frac{V}{I}\right) \times W$$

Where W is the film thickness, whose value is 224.76 nm for ZnS nanoparticles on the glass substrate, V and I are the average voltage and current of the film, respectively. The reciprocal of the resistivity was taken as the conductivity (σ) of the film.

$$\sigma = \frac{1}{\rho}$$

From the values of resistivity (ρ) and thickness (W), the sheet resistance (R_s) can be determined as

$$R_s = \frac{\rho}{W}$$

The sheet resistance for ZnS was found to be 4.83×10^7 Ω/Sq., the resistivity was calculated to be 10.85 Ω.cm, and the conductivity was also calculated to be 9.2×10^{-2} $(\Omega.cm)^{-1}$. The electrical conductivity value falls within

The magnitude of 10^{-13} to 10^2 was reported for semiconducting thin films in literature [12], suggesting that the deposited film is conductive. The observed high resistive value of the film indicates that it could find application as a semiconducting sensor.

4. Conclusion

Zinc sulphide (ZnS) nanoparticles have been successfully produced utilizing a mechanical milling technique. The ZnS nanoparticles' XRD measurements reveal peaks at the crystal plane (111), (220), (320), and (321). It was found that the ZnS nanoparticles' optical energy band gap increased from 3.72 eV to 4.02 eV. The absorbance of ZnS nanoparticles shows moderate absorbance values in the UV region but dramatically decreases as they move towards the visible and near-infrared regions. ZnS nanoparticles include 41.46% Zn, 36.79% C, 18.81% S, and 2.94 Fe, according to chemical analysis of their composition. The sheet resistance, resistivity, and conductivity were measured and found to be 4.83×10^7 Ω/Sq., 10.85 Ω.cm and 9.2×10^{-2} $(\Omega.cm)^{-1}$, respectively. ZnS nanoparticles are classified as promising materials for various optoelectronic devices based on their determined properties.

References

[1] Nicola Dengo et al., "In-Depth Study of ZnS Nanoparticle Surface Properties with a Combined Experimental and Theoretical Approach," *The Journal of Physical Chemistry C,* vol. 124, no. 14, pp. 7777-7789, 2020. *Crossref,* http://doi.org/10.1021/acs.jpcc.9b11323

[2] Xiaosheng Fang et al., "ZnS Nanostructures: From Synthesis to Applications," *Progress in Materials Science,* vol. 56, no. 2, pp. 175-287, 2011. *Crossref,* http://doi.org/10.1016/j.pmatsci.2010.10.001

[3] Xiaosheng Fang et al., "Single-Crystalline ZnS Nanobelts as Ultraviolet-Light Sensors," *Advanced Materials,* vol. 21, no. 20, pp. 2034-2039, 2009. *Crossref,* http://doi.org/10.1002/adma.200802441

[4] Xiaosheng Fang et al., "ZnO and ZnS Nanostructures: Ultraviolet-Light Emitters, Lasers, and Sensors," *Critical Reviews in Solid State and Materials Sciences,* vol. 34, pp. 190-223, 2009. *Crossref,* http://doi.org/10.1080/10408430903245393

[5] Satoshi Horikoshi, and Nick Serpone, "Introduction to Nanoparticles," *Microwaves in Nanoparticle Synthesis: Fundamentals and Applications,* pp. 1-24, 2013. *Crossref,* https://doi.org/10.1002/9783527648122.ch1

[6] Abdulkarim Z. Khalf et al., "Study of Density, Molar Volume, X-Ray Diffraction and Infrared Spectra of Phosphate Glasses," *SSRG International Journal of Applied Physics,* vol. 8, no. 2, pp. 16-20, 2021. *Crossref,* https://doi.org/10.14445/23500301/IJAP-V8I2P103

[7] Lucky I Ikhioya et al., "Influence of Dopant Concentration on the Electronic Band Gap Energy of Yb-Zrse2 Thin Films for Photovoltaic Application via Electrochemical Deposition Technique," *Materials Research Express,* vol. 7, no. 2, p. 026420, 2020. *Crossref,* https://doi.org/10.1088/2053-1591/ab7690

[8] Ihab Hassan, Mustafa Abbas Mustafa, and Basheer Elhassan, "Use of Zinc Oxide Nanoparticle for the Removal of Phenol Contaminated Water," *SSRG International Journal of Material Science and Engineering,* vol. 3, no. 2, pp. 1-5, 2017. *Crossref,* https://doi.org/10.14445/23948884/IJMSE-V3I5P101

[9] M.Jothibas et al., "Synthesis and Enhanced Photocatalytic Property of Ni Doped Zns Nanoparticles," *Solar Energy,* vol. 159, pp. 434-443, 2018. *Crossref,* https://doi.org/10.1016/j.solener.2017.10.055

[10] Yesu Thangam Y, Anitha R, and Kavitha B, "Novel Method to Synthesize and Characterize Zinc Sulphide Nanoparticle," *International Journal of Applied Sciences and Engineering Research,* vol. 1, no. 2, pp. 282-286, 2012. *Crossref,* https://doi.org/10.6088/ijaser.0020101029

[11] T.V.Arsha Kusumam et al., "Morphology Controlled Synthesis and Photocatalytic Activity of Zinc Oxide Nanostructures," *Ceramics International,* vol. 42, no. 3, pp. 3769-3775, 2016. *Crossref,* https://doi.org/10.1016/j.ceramint.2015.11.025

[12] Okafor PC, Ekpunobi AJ, and Ekwo PA, "Effect of Manganese Percentage Doping on Thickness and Conductivity of Zinc Sulphide Nanofilms Prepared by Electrodeposition Method," *International Journal of Science and Research,* vol. 4, no. 12, pp. 2275-2279, 2014.

[13] Soundararajan Thirumavalavan, Kolandavel Mani, and Suresh Sagadevan, "Investigation of the Structural, Optical and Electrical Properties of Copper Selenide Thin Films," *Materials Research,* vol. 18, no. 5, pp. 1000-1007, 2015. *Crossref,* https://doi.org/10.1590/1516-1439.039215

[14] Thirumavalavan S, Mani K, and Sagadevan S, "Studies on Structural, Surface Morphology and Optical Properties of Zinc Sulphide (Zns) Thin Films Prepared by Chemical Bath Deposition," *International Journal of Physical Sciences,* vol. 10, no. 6, pp. 204-209, 2015. *Crossref,* https://doi.org/10.5897/IJPS2015.4277

[15] Yi Xi et al., "Synthesis of ZnS Nano Flowers by Composite-Hydroxide-Mediated Approach," *Journal of Superconductivity and Novel Magnetism,* vol. 23, no. 6, pp. 901-903, 2010. *Crossref,* https://doi.org/10.1007/s10948-009-0642-y

[16] M.S.Tyagi, *Introduction to Semiconductor Materials and Devices,* John Wiley & Sons, 2018.

[17] Dai Yimin et al., "Preparation of Congo Red Functionalized Fe3O4@Sio2 Nanoparticle and its Application for the Removal of Methylene Blue," *Colloids and Surfaces A: Physicochemical and Engineering Aspects,* vol. 550, pp. 90–98, 2018. *Crossref,* https://doi.org/10.1016/j.colsurfa.2018.04.03

[18] Nwamaka I. Akpu1 et al., "Investigation on the Influence of Varying Substrate Temperature on the Physical Features of Yttrium Doped Cadmium Selenide Thin Films Materials," *SSRG International Journal of Applied Physics,* vol. 8, no. 2, pp. 37-46, 2021. *Crossref,* https://doi.org/10.14445/23500301/IJAP-V8I2P106

[19] Imosobomeh L. Ikhioyaa et al., "Effect of Precursor pHon Cadmium Doped Manganese Sulphide (CdMnS) Thin Films for Photovoltaic Application," *International Journal of Material Science and Engineering,* vol. 6, no. 2, pp. 1-8, 2020. *Crossref,* https://doi.org/10.14445/23948884/IJMSE-V6I2P101

[20] Ikhioya I. Lucky, Okoli D. N, and Ekpunobi A. J, "Effect of Temperature on SnZnSe Semiconductor Thin Films for Photovoltaic Application," *SSRG International Journal of Applied Physics,* vol. 6, no. 2, pp. 55-67, 2019. *Crossref,* https://doi.org/10.14445/23500301/IJAP-V6I2P109

[21] Ikhioya I. Lucky et al., "The Influence of Precursor Temperature on the Properties of Erbium-Doped Zirconium Telluride Thin Film Material via Electrochemical Deposition," *SSRG International Journal of Applied Physics,* vol. 7, no. 1, pp. 102-109, 2020. *Crossref,* https://doi.org/10.14445/23500301/IJAP-V7I1P115

[22] Ikhioya I. L, and A. J. Ekpunobi, "Effect of Deposition Period and pH on Electrodeposition Technique of Zinc Selenide Thin Films," *Journal of Nigeria Association of Mathematical Physics,* vol. 28, no. 2, pp. 281-288, 2014.

[23] Ikhioya I. L, and A. J. Ekpunobi, "Electrical and Structural Properties of ZnSe Thin Films by Electrodeposition Technique*," Journal of Nigeria Association of Mathematical Physics*, vol. 29, pp. 325-330, 2015.

[24] Ikhioya I. Lucky, Ugbo F. C, and Ijabor B. Okeghene, "Growth and Characterization of Manganese Sulphide (MnS) Thin Films," *International Journal for Research in Applied and Natural Science*, vol. 4, no. 1, pp. 1-9, 2018.

[25] Navneet Kaur et al., "A Review on Zinc Sulphide Nanoparticles: From Synthesis, Properties to Applications," *Journal of Bioelectronics and Nanotechnology*, vol. 1, no. 1, pp. 1-5, 2016.